JOURNAL OF PROPULSION AND POWER
Vol. 18, No. 2, March–April 2002

# Combustion Instability Active Control Using Periodic Fuel Injection

J. P. Hathout*
*Robert Bosch Corporation, Palo Alto, California 94304*
M. Fleifil†
*John Zink Company, Tulsa, Oklahoma*
and
A. M. Annaswamy‡ and A. F. Ghoniem§
*Massachusetts Institute of Technology, Cambridge, Massachusetts 02139*

**Active control using periodic fuel injection has the potential of suppressing combustion instability without radically changing the engine design or sacrificing performance. A study is carried out of optimal model-based control of combustion instability using fuel injection. The model developed is physically based and includes the acoustics, the heat-release dynamics, their coupling, and the injection dynamics. A heat-release model with fluctuations in the flame surface area, as well as in the equivalence ratio, is derived. It is shown that area fluctuations coupled with the velocity fluctuations drive longitudinal modes to resonance caused by phase-lag dynamics, whereas equivalence ratio fluctuations can destabilize both longitudinal and bulk modes caused by time-delay dynamics. Comparisons are made between the model predictions and several experimental rigs. The dynamics of proportional and two-position (on–off) fuel injectors are included in the model. When the overall model is used, two different control designs are proposed. The first is an linear quadratic Gaussian/loop transfer recovery controller, where the time-delay effect is ignored, and the second is a positive forecast controller, which explicitly accounts for the delay. Injection at 1) the burning zone and 2) farther upstream is considered. The characteristics of fuel injectors including bandwidth, authority (pulsed-fuel flow rate), and whether it applies a proportional or a two-position (on–off) injection are discussed. We show that increasing authority and increasing bandwidth result in improved performance. Injection at location 2 compared to location 1 results in a tradeoff between improved mixing and increased time delay. It is also noted that proportional injection is more successful than on–off injection because the former can modulate both amplitude and phase of the control fuel.**

## Nomenclature

| | | |
|---|---|---|
| $A_c$ | = | cross-sectional area of the combustor |
| $A_e$ | = | inlet cross-sectional area of the slug flow |
| $A_f$ | = | flame area |
| $A_i$ | = | outlet cross-sectional area of the slug flow |
| $B_e$ | = | magnetic flux density |
| $b$ | = | damping of the armature/poppet |
| $c$ | = | speed of sound |
| $E$ | = | voltage |
| $F_m$ | = | magnetic force |
| $i$ | = | current |
| $k$ | = | stiffness of the armature/poppet |
| $k_p$ | = | gain of the combustor transfer function |
| $L$ | = | length of the slug flow |
| $L_c$ | = | distance between injector and burning zone |
| $L_e$ | = | inductance of the coil |
| $L_i$ | = | distance between tank and valve's outlet |
| $l$ | = | length of the armature |
| $m$ | = | mass of the armature/poppet |
| $\dot{m}$ | = | mass flow rate of gas |
| $\bar{m}_a$ | = | mean air mass flow rate |
| $p$ | = | pressure |
| $\tilde{p}\%$ | = | pressure reduction rate |
| $Q$ | = | total heat release rate |
| $q$ | = | heat release rate per unit area |
| $R_e$ | = | resistance of the solenoid coil |
| $R_m(s)$ | = | desired characteristic equation |
| $R_p(s)$ | = | denominator of combustor transfer function |
| $S_u$ | = | burning velocity |
| $u$ | = | velocity |
| $u_s$ | = | velocity at fuel supply |
| $V$ | = | volume of the cavity |
| $W_p(s)$ | = | TF of combustor |
| $x$ | = | motion of armature |
| $Z_p(s)$ | = | numerator of combustor transfer function |
| $\alpha_0$ | = | stoichiometric fuel to air ratio |
| $\Delta h_r$ | = | heat of reaction |
| $\zeta$ | = | passive damping ratio in combustor |
| $\eta(t)$ | = | modal basis function |
| $\xi(r, t)$ | = | axial displacement of flame |
| $\rho_u$ | = | density of the unburnt mixture |
| $\tau_c$ | = | convective delay |
| $\tau_e$ | = | armature electric time constant |
| $\tau_f$ | = | characteristic propagation delay |
| $\tau_{\text{fluid}}$ | = | fluidic time constant |
| $\phi$ | = | equivalence ratio |
| $\phi_m$ | = | normalized equivalence ratio perturbation |
| $\psi(x)$ | = | modal basis function |

*Superscripts*

| | | |
|---|---|---|
| $\bar{}$ | = | steady quantity |
| $'$ | = | perturbation quantity |

Received 23 July 2000; revision received 24 October 2001; accepted for publication 25 October 2001. 

*Project Manager, Research and Technology Center.
†Acoustics Engineer, Technology and Commercial Development Group.
‡Principal Research Scientist, Department of Mechanical Engineering.
§Professor, Department of Mechanical Engineering. Associate Fellow.

## I. Introduction

COMBUSTION instability has been widely observed in premixed combustion at near-stoichiometric operation in high-power combustors,[1–4] as well as at lean near-flammability conditions in low-emission combustors.[5–7] Active control has been recognized as a promising technology to abate combustion instability in practical systems.[5,7–11] Among the various methods, control using periodic fuel injection has been observed to have the maximum impact on instability using the smallest fraction of the system energy. A systematic active control design for pulsing fuel that can guarantee optimal and robust performance over a wide range of operating conditions is, therefore, highly desirable.

It has long been recognized that combustion instability is governed by strong coupling between the heat release and the acoustic field of the combustor chamber.[12] Although acoustics is well known and can be modeled accurately,[13] heat-release dynamics remains a challenge. Most current designs are based on phase-shift algorithms that succeed over a small range of operating conditions where the frequency and phase characteristics do not vary significantly. In addition, their behavior is not optimal in terms of fuel consumption, settling time, and robustness. To design an efficient active controller that can deliver guaranteed performance, a model of the actuated combustor that includes the combustion instability and the underlying dominant interactions between acoustics and the heat release, the actuator dynamics such as its bandwidth, nonlinearities, authority, delay effects, and effects of operating conditions, actuator type, and actuator locations is highly desirable. In this paper, we develop a general model of the acoustics, heat release, and fuel injector and various interactions between these components.

The response of heat-release rate for various perturbations in the flowfield is slowly beginning to be understood. Of these, perturbations due to velocity and equivalence ratio are two mechanisms that appear to affect heat-release rate in a dominant way. The heat-release response to perturbations in the velocity through area fluctuations was first quantified by Fleifil et al.[14] to establish a reduced-order model of combustion instability[15] in a laminar flow and was later adopted by Peracchio and Proscia[16] and Dowling[17] to establish instability under more turbulent conditions. The heat-release response to perturbations in the equivalence ratio was observed experimentally in Refs. 18–20, with preliminary results related to their modeling reported in Refs. 21 and 22. Whereas both mechanisms can destabilize longitudinal modes,[9,19,23,24] bulk modes are more strongly affected by the latter.[8,21] In this paper, we derive a general heat-release model that captures the effect of both velocity and equivalence ratio perturbations. We use the same flame kinematics equation as in Ref. 14 and derive a reduced-order model of the heat-release dynamics assuming that we have conditions of high Damkohler number, that there is weak to moderate turbulent intensity, and that it is a thin sheet separating reactants and products. The acoustic modes are assumed to be either due to a bulk mode or a longitudinal mode. Coupling the heat-release model and the acoustics, we derive the instability conditions for the combustor. We show that two different perturbations can cause the instability, where the first is due to equivalence ratio fluctuations and a convective delay, whereas the second is due to velocity fluctuations and a propagative time delay. The model predictions in the first category are compared to experimental rigs in Refs. 8, 9, 20 and 25, whereas those in the second are compared to Refs. 9, 23, and 26–28.

The performance of the active controller is tightly correlated with the performance of sensors and actuators. Whereas high-bandwidth devices of the first are available, for example, pressure transducers and heat-release sensors, actuation by means of fuel injection consists of low-bandwidth, limited authority, time delays and nonlinearities (in the form of dead-zone, saturation, and on–off effects).[29] Therefore, it is important to model these effects and to include them as much as possible in the control design. The impact of ideal actuators on combustion dynamics was studied extensively by Hathout et al.,[30] where it was assumed that the actuator has a very high bandwidth and is free of nonlinearities as well as time delay. In this paper, we study the effect of all of the mentioned deviations from the ideal case. The most dominant effect of the actuator dynamics is a time delay, which occurs due to the distance of the injection location from the burning plane. This effect is modeled explicitly and taken into account in the control design. When the combined model of the combustion dynamics and the fuel-injector model is used, two different control designs are proposed in this paper, which include 1) a linear quadratic gaussian/loop transfer recovery (LQG/LTR) controller and 2) a positive forecast (Posi-Cast) controller. The former is utilized for the case when the injection is at the burning zone because the time delays present are small, whereas the latter is relevant when the injector is upstream of the burning zone because it introduces significant delays. In all cases, the impact of bandwidth, authority, and nonlinearities is investigated.

## II. Physically Based Combustor Model

In this section, we model the combustor heat release, acoustics, and inhomogeneity dynamics, and we investigate the coupling between these dynamics and the susceptibility to instability.

### A. Heat-Release Dynamics

Modeling of the heat release dynamics is a challenge that has been clouded by the intricacy of turbulent combustion. One way of alleviating the complexity is by modeling turbulent premixed combustion at high Damkohler numbers and weak to moderate turbulence intensity as wrinkled laminar flames.[2] This was done by Fleifil et al.[14] to quantify the heat-release response to perturbations in the velocity through area fluctuations. We carry out a similar procedure, where we address the effects of perturbations in the equivalence ratio in addition to the velocity perturbations. As in Ref. 14, the following assumptions are made to derive our model: 1) The flame is a thin interface separating reactants and products and is insensitive to pressure perturbations.[5] 2) The flame can model turbulent premixed combustion if conditions of high Damkohler number and weak to moderate turbulence intensity prevail.[2,16,31] 3) The flame is weakly convoluted.

Under these assumptions, the flame surface can be described by a single-valued function $\xi(r, t)$, which represents the instantaneous axial displacement of the flame, and the total heat release $Q$ is proportional to the integral of this surface over an anchoring ring:

$$\frac{\partial \xi}{\partial t} = u - v\frac{\partial \xi}{\partial r} - S_u(\phi)\sqrt{\left(\frac{\partial \xi}{\partial r}\right)^2 + 1} \tag{1}$$

$$Q = \kappa(\phi)\int_0^R \sqrt{1 + \left(\frac{\partial \xi}{\partial r}\right)^2}\,\mathrm{d}r \tag{2}$$

where $\kappa(\phi) = 2\pi\rho_u S_u(\phi)\Delta h_r(\phi)$. (We consider here a flame stabilized over a perforated plate; $R$ is the radius of the perforation.) To derive a linear model, the effects of perturbations in both $u$ and $\phi$ will be considered.

Assuming negligible velocity component in the radial direction and linearizing around nominal values $\bar{u}$, $\bar{S}_u$, and $\bar{\xi}(r)$, we get

$$\frac{\partial \xi'}{\partial t} = u' + \bar{S}_u\frac{\partial \xi'}{\partial r} + \frac{\partial \bar{\xi}}{\partial r}\left.\frac{\mathrm{d}S_u}{\mathrm{d}\phi}\right|_{\bar{\phi}}\phi' \tag{3}$$

where $\bar{u} > S_u$ and the boundary conditions

$$\xi'(R, t) = 0\,\forall\, t, \qquad \xi'(r, 0) = 0\,\forall\, r \tag{4}$$

[Note that with the appropriate change in coordinates and boundary conditions, Eq. (3) can also represent flames stabilized behind a gutter[17] or a dump.[16]] Similarly, the unsteady heat release can be linearized by considering, in addition to finite $u'$, perturbations in $\Delta h_r$ and $S_u$ due to $\phi'$ to obtain the relation

$$Q'(t) = \bar{\kappa}\int_0^R \xi'(r, t)\,\mathrm{d}r + d_\phi\phi' \tag{5}$$

where

$$\bar{\kappa} = 2\pi\rho_u S_u \Delta\bar{h}_r$$

$$d_\phi = 2\pi\rho_u \left( \bar{S}_u \frac{\mathrm{d}\Delta h_r}{\mathrm{d}\phi}\bigg|_{\bar{\phi}} + \Delta\bar{h}_r \frac{\mathrm{d}S_u}{\mathrm{d}\phi}\bigg|_{\bar{\phi}} \right) \left( \int_0^R r\bar{\xi}\,\mathrm{d}r \right)$$

(The factor $\mathrm{d}\Delta h_r/\mathrm{d}\phi|_{\bar{\phi}}$ is positive, and $\mathrm{d}S_u/\mathrm{d}\phi|_{\bar{\phi}}$ is also positive when $\phi \le 1$.)

Note that the flame area fluctuation $A'_f$ is given by

$$A'_f(t) = 2\pi \int_0^R \xi'(r,t)\,\mathrm{d}r$$

This, with Eq. (3), shows that the flame area is affected by both $u'$ and $\phi$ and that the area in turn impacts $Q'$ as shown in Eq. (5). This also shows that $\phi'$ affects $Q'$ directly and indirectly through the area fluctuations.

Equation (3) can be manipulated further and solved for $\xi'$ in the Laplace domain as

$$\xi'(r,s) = \left( \frac{u'(s)}{s} + \frac{\partial\bar{\xi}}{\partial r}\frac{\mathrm{d}S_u}{\mathrm{d}\phi}\bigg|_{\bar{\phi}} \frac{\phi'(s)}{s} \right) \left\{ 1 - \exp\left[ -(R-r)\frac{s}{\bar{S}_u} \right] \right\} \tag{6}$$

where $s$ is the Laplace operator. Differentiating Eq. (5) with respect to time and using Eq. (3), we get

$$\dot{Q}' = \bar{\kappa} \int_0^R \left( u' + \bar{S}_u \frac{\partial\xi'}{\partial r} + \frac{\partial\bar{\xi}}{\partial r}\frac{\mathrm{d}S_u}{\mathrm{d}\phi}\bigg|_{\bar{\phi}} \phi' \right) \mathrm{d}r + d_\phi \dot{\phi}' \tag{7}$$

which is integrated over $r$ as

$$\dot{Q}' = \bar{\kappa} \left( Ru' - \bar{S}_u \xi'(0,t) + \int_0^R \frac{\partial\bar{\xi}}{\partial r}\frac{\mathrm{d}S_u}{\mathrm{d}\phi}\bigg|_{\bar{\phi}} \phi'\,\mathrm{d}r \right) + d_\phi \dot{\phi}' \tag{8}$$

Taking the inverse Laplace of Eq. (6) at $r = 0$ and substituting in Eq. (8), after some manipulations we get

$$\dot{Q}' = d_0 u' + d_1 \left[ u'_{\tau_f}(t) \right] + d_2 \left[ \phi'_{\tau_f}(t) \right] + d_3 \phi' + d_\phi \dot{\phi}' \tag{9}$$

where

$$x_\tau(t) \triangleq \int_{t-\tau_f}^{t} x(\zeta)\,\mathrm{d}\zeta, \qquad d_0 = \bar{\kappa} R, \qquad d_1 = -\bar{\kappa}\bar{S}_u$$

$$d_2 = -\bar{\kappa}\bar{S}_u \frac{\partial S_u}{\partial\phi}\bigg|_{\bar{\phi}} \frac{\partial\xi(r)}{\partial r}\bigg|_0, \qquad d_3 = -\bar{\kappa}\frac{\partial\bar{S}_u}{\partial\phi}\bar{\xi}(0)$$

$$\bar{\kappa} = 2\pi\rho\Delta h_r \bar{S}_u, \qquad \tau_f = \frac{R}{\bar{S}_u} \tag{10}$$

where $\tau_f$ is the characteristic propagation delay of the flame surface into the reactants flow. Note that, for the class of flames considered in the paper, the slope at the flame tip, which is typically conical, is zero, and therefore, the third term on the right-hand-side of Eq. (9) can be omitted. We also note that, if the dominant instability is due to the bulk mode, it implies that the velocity fluctuations $u'$ are zero. Hence, unsteady heat release can occur only if equivalence ratio perturbations are present, for weak to moderate turbulent intensity.

### B. Acoustics

The host oscillators responsible for the combustion instability, in most cases, are generated by resonant acoustic modes. These are, typically, Helmholtz-type, longitudinal or transverse, with the type of mode determined by the geometry of the combustion chamber. Helmholtz-type combustion instabilities (also known as bulk-mode instabilities) are characterized by low frequencies and no spatial dependence for the pressure, unlike longitudinal modes, which resonate at higher frequencies and vary with the span of the combustor depending on the boundary conditions.[24] Both bulk and longitudinal modes coexist in many rigs.[8,28,29,32]

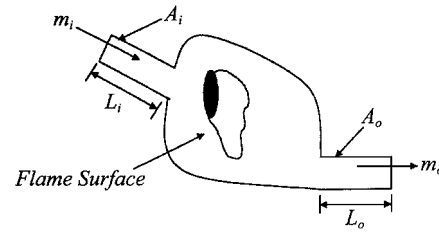


**Fig. 1 Schematic diagram of a combustor exhibiting a Helmholtz-type resonance.**

The origin of a Helmholtz-type resonance[13] is the coupling between a compressible volume of gas in a large cavity creating a restoring potential energy for an oscillating mass of slug flow gas in a narrow neck attached to the cavity. The slug flow could occur either at the inlet or exit piping to the combustor chamber where the flame resides and that can be considered as the cavity (see Fig. 1).

The governing equations of the Helmholtz-mode are derived formally by using the following assumptions: 1) The flow is assumed one dimensional and incompressible in the ducts. 2) The volume of the combustor chamber is larger than that of each duct. 3) The gas behaves as a perfect gas and is inviscid. When the mass and energy conservations in the combustor portrayed in Fig. 1 are applied, and the perfect gas state equation is used, the perturbation of the pressure in the combustor cavity around the steady mean can be evaluated as

$$\frac{\mathrm{d}p'}{\mathrm{d}t} = \frac{1}{V}\left[ c_i^2 \dot{m}'_i - c_e^2 \dot{m}'_e + (\gamma - 1)Q' \right] \tag{11}$$

where the subscripts $i$ and $e$ denote inlet and exit, respectively. When momentum and mass conservation are used, the perturbed incompressible flow in the ducts satisfies

$$\frac{\mathrm{d}\dot{m}'_j}{\mathrm{d}t} = -A_j \frac{\partial p'_j}{\partial x}(L_j, t) \tag{12}$$

where $A$ and $L$ are the cross-sectional area and length of the slug flow in the $j$th duct and $j = i$ or $e$. By substitution in Eq. (11), we get

$$\frac{\mathrm{d}^2 p'}{\mathrm{d}t^2} + \frac{1}{V}\left[ c_i^2 A_i \frac{\partial p'_i}{\partial x}(L_i, t) - c_e^2 A_e \frac{\partial p'_e}{\partial x}(L_e, t) \right] = \frac{\gamma - 1}{V}\frac{\mathrm{d}Q'}{\mathrm{d}t} \tag{13}$$

When the inlet and the exit ducts are assumed acoustically open to the atmosphere, that is, the pressure distribution in the ducts is negligible, then, $(\partial p'_j/\partial x)(L_j, t) = p'/L_j$, and this results in the following oscillator equation for the pressure in the combustor:

$$\frac{\mathrm{d}^2 p'}{\mathrm{d}t^2} + 2\zeta\omega\frac{\mathrm{d}p'}{\mathrm{d}t} + \omega^2 p' = \frac{\gamma - 1}{V}\dot{Q}' \tag{14}$$

where $\omega = \sqrt{[(c_i^2 A_i/L_i V) + (c_e^2 A_e/L_e V)]}$ is the effective Helmholtz frequency[13] associated with a combustor connected to ducts. The passive damping in the combustor due to different dissipation sources, for example, heat loss and friction, is accounted for in the natural damping ratio $\zeta$.

The governing equations for a longitudinal mode can be derived in a straightforward manner[24] and are of the form

$$\frac{\partial^2 p'}{\partial t^2} - \bar{c}^2 \frac{\partial^2 p'}{\partial x^2} = (\gamma - 1)\dot{q}'(x,t) \tag{15}$$

where $\bar{c}$ is the mean speed of sound and $q'$ is the heat release rate per unit volume.

Equations (14) and (15) denote the acoustic dynamics for a Helmholtz mode and a longitudinal mode, respectively. In what follows, instabilities arising from either of these two modes will be

considered. The same approach can be used for transverse modes as well, for example, screech modes in rockets.[33] We also assume that flames are localized close to the anchoring plane, so that $q'(x,t) = [Q'(t)/A_c]\delta(x - x_f)$.

By the use of an expansion in basis functions for both Eqs. (14) and (15) as

$$p'(x,t) = \bar{p}\sum_{i=0}^{n} \psi_i(x)\eta_i(t) \tag{16}$$

where $\psi_0$ is a constant, because it corresponds to the spatial variation in the bulk mode, $\psi_i(x) = \sin(k_i x + \phi_{i0})$, $i = 1, \ldots, n$, and $k_i$ and $\phi_{i0}$ are determined from the boundary conditions. Performing a weighted spatial averaging, the modal amplitudes can be shown to follow[24]

$$\ddot{\eta}_i + 2\zeta\omega_i\dot{\eta}_i + \omega_i^2\eta_i = \sum_{i=1}^{n} \tilde{b}_i\dot{Q}' \tag{17}$$

where $\tilde{b}_0 = \gamma - 1/V$, $\tilde{b}_i = \gamma a_0 \psi_i(x_f)/(A_c E)$ for $i = 1, \ldots, n$,

$$E = \int_0^L \psi_i^2(x)\,\mathrm{d}x$$

where $\gamma$ is the specific ratio, $a_0 = (\gamma - 1)/\gamma\bar{p}$, $\zeta$ is the damping ratio, $L$ is its length, $\omega_0^2 = \sqrt{(A_n/L_n V)}$, $V$ is the volume of the combustor, $A_n$ and $L_n$ are the cross-sectional area and length of the inlet/outlet neck connected to the combustor, and $\omega_i = k_i\bar{c}$, $i = 1, \ldots, n$. Typically, $\omega_0 \ll \omega_i$, for $i = 1, \ldots, n$. (Note that dissipation in a combustor can be caused by heat losses in the flame zone and friction due to viscous effects.)

### C. Coupling Dynamics

In Secs. II.A and II.B, we analyzed heat release and acoustics individually. Here, we investigate the physical coupling between the heat release and the acoustics, which will drive them to resonance.

In the case when a Helmholtz-type resonance is triggered in the combustor, the acoustic velocity is very small in the bulk, and the possible coupling between heat release fluctuations and acoustics is through the pressure. Under such conditions, we can assume that $u' \sim 0$ (Ref. 22). However, coupling can be produced through perturbations in the equivalence ratio, which in turn can occur due to feedline dynamics.[16] In particular, if either the air- or fuel-flow feed is choked and the other feed is unchoked, $\phi$ can fluctuate. In general, the fuel nozzle is more likely to be choked than the air duct,[16] and the instantaneous equivalence ratio $\phi_s$ at the exit of the fuel nozzle due to airflow fluctuations is determined as

$$\phi_s = \bar{\phi}/(1 + u_s'/\bar{u}) \tag{18}$$

where $u_s$ is similar to a relation used in Ref. 16. When linearized, we obtain the following relation:

$$\phi' = -(\bar{\phi}/\bar{u})u' \tag{19}$$

In addition, there is a convective delay $\tau_c$ due to transport lag from the supply to the burning plane of the flame, and, hence,

$$\phi' = \phi_s'(t - \tau_c) \tag{20}$$

where $\tau_c = L/\bar{u}$.

The equivalence ratio perturbations, in turn, can be related to the pressure perturbations in the combustor by considering the momentum conservation in the inlet duct,

$$\frac{\partial u_i'}{\partial t} + \frac{1}{\rho_i}\frac{\partial p_i}{\partial x} = 0 \tag{21}$$

where $u_i$ and $p_i$ are the velocity and the pressure at the inlet duct, respectively. When the dominant acoustic modes are longitudinal, both perturbations in $u$ and $\phi$ can induce instability. The coupling between $u$ and $p$ can be determined using the energy conservation equation as

$$\frac{\partial p'}{\partial t} + \gamma\bar{p}\frac{\partial u'}{\partial x} = (\gamma - 1)q' \tag{22}$$

### D. Complete Combustion Model

Combining the acoustics, heat-release, and convective-lag effects, we obtain the following equations:

$$\ddot{\eta}_i + 2\zeta\omega_i\dot{\eta}_i + \omega_i^2\eta_i = \tilde{b}_i\left\{d_0 u' + d_1\left[u'_{\tau_f}(t)\right] + d_2\left[\phi'_{\tau_f}(t)\right] + d_3\phi'(t - \tau_c) + d_\phi\dot{\phi}'(t - \tau_c)\right\} \tag{23}$$

Equation (23) indicates that two different time delays, $\tau_f$ and $\tau_c$, can induce these excitations, one arising from propagation effects and the other from convection. Also note from Eq. (23) that if the dominant pressure mode is that of a bulk mode then it can be excited only due to perturbations in the equivalence ratio. However, if longitudinal modes are the ones that are dominant, they can be excited either by $u'$ perturbations or by $\phi'$ perturbations.

The complete combustion dynamics is, therefore, determined by Eq. (23) and the coupling relations given by Eqs. (20–22). For ease of exposition, we assume that only one acoustic mode is present and set $\eta_i = \eta$. Equation (20) or Eqs. (21) and (22) are used, depending on whether the dominant variations are in $u'$ or in $\phi'$. If the variations are mainly in $u'$, then Eqs. (23) and (22) can be combined to obtain the relation

$$\ddot{\eta} + (2\zeta\omega - \gamma_1)\dot{\eta} + \left(\omega^2 + \gamma_2\right)\eta - \gamma_2\eta(t - \tau_f) = 0 \tag{24}$$

where

$$\gamma_1 = \bar{\kappa}R\tilde{b}\tilde{c}, \qquad \gamma_2 = \bar{\kappa}\tilde{S}_u\tilde{b}\tilde{c}, \qquad \tilde{c} = \frac{1}{\gamma k^2}\frac{\mathrm{d}\psi}{\mathrm{d}x}\bar{p}, \qquad \tilde{b} = \tilde{b}_1$$

and if they are due to $\phi'$, then Eqs. (23), (21), and (20) can be combined to obtain

$$\ddot{\eta} + 2\zeta\omega\dot{\eta} + \omega_i^2\eta - \beta_1\eta(t - \tau_c) + \beta_2\eta_i(t - \tau_c) - \beta_3\eta_{i_{\tau_f}} = 0$$

$$\eta_i(t) = \int_0^t \eta(\zeta)\,\mathrm{d}\zeta \tag{25}$$

where

$$\beta_1 = 2\pi\rho_u\tilde{b}\frac{\bar{\phi}}{\bar{u}}\tilde{c}\gamma k^2\left(\bar{S}_u\frac{\mathrm{d}\Delta h_r}{\mathrm{d}\phi}\bigg|_{\bar{\phi}} + \Delta\bar{h}_r\frac{\mathrm{d}S_u}{\mathrm{d}\phi}\bigg|_{\bar{\phi}}\right)\left(\int_0^R r\bar{\xi}\,\mathrm{d}r\right)$$

$$\beta_2 = 2\pi\rho_u\tilde{b}\frac{\bar{\phi}}{\bar{u}}\tilde{c}\gamma k^2\Delta\bar{h}_r\bar{S}_u\frac{\mathrm{d}\bar{S}_u}{\mathrm{d}\phi}\bar{\xi}(0)$$

$$\beta_3 = -\tilde{b}\frac{\bar{\phi}}{\rho\bar{u}}\tilde{c}\gamma k^2\bar{\kappa}\bar{S}_u\frac{\mathrm{d}\bar{S}_u}{\mathrm{d}\phi}$$

At the acoustic frequency, the impact of the second term on the right-hand side of Eq. (25) is typically smaller. Hence, a simplified version of Eq. (25) can be analyzed in the form

$$\ddot{\eta} + 2\zeta\omega\dot{\eta} + \omega^2\eta - \beta_1\eta(t - \tau_c) = 0 \tag{26}$$

Note that the structure of Eq. (26) is identical to that of Eq. (24) with the differences only due to the parameters. The other distinction is in the damping effect; in the former, if $\gamma_1$ is positive, even in the absence of any time delay, instabilities can be present. In the latter, on the other hand, instability is only due to the time delay $\tau_c$; the damping effect is stabilizing.

The preceding discussions indicate that the general class of models that describe the combustion instability are of the form of

$$\ddot{\eta} + 2\zeta_0\omega\dot{\eta} + \left(\omega^2 - k_1\right)\eta + k_2\eta(t - \tau) = 0 \tag{27}$$

with $\zeta_0, \omega, k_1, k_2$, and $\tau$ taking different values depending on whether the instability is due to $u'$ or $\phi'$.

## III. Instability Properties and Comparison with Experimental Results

In Ref. 34, stability bounds for both second-order and third-order delayed ordinary differential equations of the form of Eqs. (27) and (25), respectively, were investigated. The highlights of Ref. 34 that are relevant for our discussions here are briefly stated.

For a system of the form of Eq. (27), three possibilities exist: 1) the system is always stable for all $\tau$, 2) the system is stable for $\tau \in [0, \tau^*]$ and unstable for all $\tau \geq \tau^*$, and 3) the system alternates between stability and instability as $\tau$ increases. The results of Ref. 34 outline conditions on the parameters $\zeta$, $\omega$, $k_1$, and $k_2$, for cases 1–3 to occur. For case 3, it is necessary for $k_1 < \omega^2$ . In most combustors, it can be shown that the latter is satisfied, that is, one should expect the presence of instability bands. Note that most experimental results where $\phi'$ fluctuations occur illustrate such bands. We now make more detailed comparisons between the bands predicted by our model and experimental results.

### A. Instability due to $\phi'$ Fluctuations

We now compare the instability characteristics predicted by the model in Eq. (27) with the four experimental results presented in Refs. 8, 19, 20, and 25. In the first three cases, the fuel feedline was choked while that of air was unchoked. In Ref. 20, Lieuwen and Zinn also studied the case when the fuel line was unchoked and the air feed was choked. In Ref. 25, the corresponding details are not given, though fluctuations were observed to be present at the outlet of the fuel line. Such feedline characteristics introduce $\phi'$ fluctuations, as shown in Sec. II.C. We consider each of these four results and show how the instability characteristics as predicted by the model in Eq. (27) compare with the results reported in Refs. 8, 9, 20, and 25.

In Ref. 20, measurements of the pressure amplitude from different experiments where the position of the unchoked fuel inlet was changed, hence changing the convective delay $\tau_c$, were collected as a function of $\tau_c/\tau_{ac}$, where $\tau_{ac} = 2\pi/\omega$. The unstable regimes cluster around $\tau_c/\tau_{ac} = 0.65$ and 1.6, which is in agreement with our model. We neglected the effect of damping in all four cases, because it is small and difficult to quantify. The results in Ref. 34 show that instability occurs when

$$(n+1)/2 < \tau_c/\tau_{ac} < (n+2)/2 \qquad \text{for } n = 0, 2, 4, \ldots \tag{28}$$

which encompasses the unstable regions in Ref. 20. In addition, in Ref. 19, instability occurred at $0.5 < \tau_c/\tau_{ac} < 1.0$, when the fuel inlet was unchoked, which is in agreement with our model predictions (Fig. 2). Note that the acoustic mode was that of a quarter-wave in Ref. 19 and a half-wave in Ref. 20.

The instability mode in Ref. 8 corresponds to that of a bulk mode with $\omega = 200$ Hz, where $\phi'$ fluctuations were measured. Based on the experimental data provided in Ref. 8, we calculated $\tau_c = 3.1$ ms, leading to $\tau_c/\tau_{ac} = 0.62$, which matches the model predictions from Eq. (28).

Our final comparison is with the results by Mongia et al.,[25] where the instability characteristics were observed to vary with $L$, the distance of the fuel injector from the burning zone (see Fig. 7 in Ref. 25). The paper shows that instability is also dependent on the value of $\bar{\phi}$. As the latter decreases, the instability vanishes. Our model can predict this behavior because $\bar{\phi}$ affects $\beta_1$ in Eq. (26). According to Ref. 34, as $\bar{\phi}$ and, hence, $\beta_1$ decreases, and below a critical value for the latter, the system will be stable irrespective of the amount of delay.

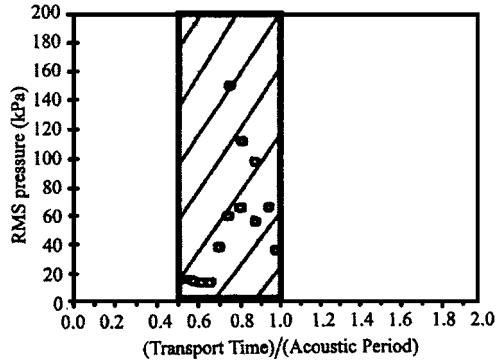


**Fig. 2 Instability band measured in Ref. 19 vs our model predictions (shaded area).**

### B. Instability due to $u'$ Fluctuations

In several other experimental studies[9,23,26–28,35] the feedline dynamics was decoupled from the burning zone, but the pressure instabilities were still observed to be present. In this section, we compare our model predictions with the results from these studies. The results in Refs. 23, 26, and 27 pertain to laminar flow conditions, with the air and fuel thoroughly mixed before the burning zone, which allows one to assume that $\phi'$ fluctuations are small. In Ref. 28, the fuel- and airstreams are introduced using similar means with neither being choked. In Ref. 9, a premixer upstream of the cold section of the combustor was introduced to ensure thorough mixing. In Ref. 36, a similar arrangement is made to decouple the feedline perturbations. That is, in all of these experimental studies, thorough mixing was achieved, and as a result, it is reasonable to assume that $\phi'$ perturbations are small. However, in these studies, combustion instabilities were still observed to be present, which indicate that a mechanism different from $\phi'$ fluctuations may be responsible for the resonance.

As mentioned in Sec. II.D, two different perturbations, $u'$ and $\phi'$, can result in instability, as represented by the models in Eqs. (24) and (25), respectively. The model in Eq. (24) and the discussion in Sec. III show that 1) if $\gamma_1 > 0$, instability can be present for very small values of $\tau_f$ and 2) as the time delay $\tau_f$ in Eq. (24) increases, the system can alternate between stability and instability.

We now evaluate the model properties 1 and 2 through the studies of Refs. 9, 23, 26–28, and 35. In Refs. 23, 26, and 27, the three-quarter mode is dominant, for which $\gamma_1 > 0$. The experiments reveal that this mode is unstable, which corroborates property 1. In these studies, $\tau_f$ is negligible because the flow velocities are in the laminar region, and hence, $R/S_u$ is small. Hence, the operating condition falls always in the first band, which corresponds to instability. Therefore, property 2 is indirectly validated.

In Refs. 9, 28, and 35, the flow velocities are in the turbulent regime. The question here is whether the model in Eq. (27) can predict the instability reported in these three papers. Clearly, other mechanisms, especially those due to hydrodynamics and vortex–flame interactions, are present and may contribute to the instability. Therefore, parameters such as $\tau_f$ in model (24) may not be physically meaningful. However, note that the global instability properties of the model such as properties 1 and 2 are mirrored in the experiments in Refs. 9, 28, and 35. In Refs. 9 and 28, the quarter-wave mode of the hot section is driven to resonance. This implies that $\gamma_1$ in Eq. (24) is negative, and hence, $\zeta_0$ in Eq. (27) is positive. However, instability bands were observed to occur in Ref. 9 as $\bar{\phi}$ changes. Noting that $\tau_f$ is a function of $S_u$ and, therefore, a function of $\bar{\phi}$, property 2 can be viewed as a corroboration of the results by Richards et al.[9] In Ref. 35, the half-wave mode is dominant, for which $\gamma_1 > 0$, and hence, property 2 corroborates the results by Kim et al.[35] as well, albeit indirectly.

## IV. Control

In this section, we investigate model-based control strategies for abating combustion instability using secondary fuel injection. A pulsating fuel injector delivers oscillations in the mass flow rate in response to a voltage input. The injector dynamics is modeled from first principles, both in the case when the mass flow rate is proportional to the input voltage and in the case when the injector operates in an on–off mode. We assume that the pressure signal is the measured output, using a pressure transducer. The transducer dynamics is neglected because it typically has a much higher bandwidth than the combustion dynamics. We then develop active control strategies using the model developed in Sec. II for the combustion dynamics and the fuel-injector model. We study the cases where an injector is located at 1) the burning zone or 2) farther upstream. We assume that

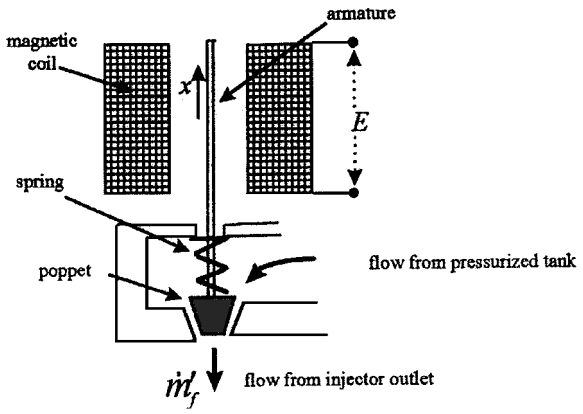


**Fig. 3 Schematic of typical injector.**

the combustion dynamics is determined by several coupled acoustic modes.[24] The control design is carried out for the case when the instability is primarily induced by fluctuations in the flame area coupled with the acoustics. See Refs. 21 and 22 for investigationsof instability caused by equivalence ratio fluctuations and its control.

### A. Fuel-Injector Dynamics

*1. Proportional Injector*

The injector system consists of an electromechanical part and a fluidic part, where, in the former, the input voltage generates an electromagnetic field that causes a poppet to move against a spring (Fig. 3). The motion of the poppet controls the aperture of the injector allowing fluid to flow.

The electromechanical part relates the voltage $E$ to the poppet position $x$ through the electrical, electromagnetic, and mechanical components, which can be modeled as

$$E = iR_e + L_e\frac{\mathrm{d}i}{\mathrm{d}t} + V \tag{29}$$

$$V = B_e l\frac{\mathrm{d}x}{\mathrm{d}t} \tag{30}$$

$$F_m = B_e l i \tag{31}$$

$$m\frac{\mathrm{d}^2x}{\mathrm{d}t^2} + b\frac{\mathrm{d}x}{\mathrm{d}t} + kx = F_m \tag{32}$$

where $x$ is the motion of the armature in the direction of the magnetic force, $l$ is the length of the armature, which moves orthogonal to the magnetic field, respectively. Here, $m$ is the effective mass.

In most solenoid systems, the armature electric time constant, $\tau_e = L_e/R_e$, is negligible compared to the acoustics time constant.[36] In these valves, the stiffness of the spring, $k$, is large, for a fast closing of the valve, when the voltage is turned off. Also, the mass $m$ of the armature is very small in many of the typical injectors to minimize inertia forces.[36] The damping term $b$ contains the overall damping, including stiction and friction, and typically is large. Thus, the mechanical system can be simplified as a first-order, damper–spring system.[37] The mechanical time constant usually limits the bandwidth of typical injectors to approximately 100 Hz. (Note that other effects, such as impact dynamics, are not included here because we expect them to be of higher frequencies than the combustor dynamics.)

Thus, Eqs. (29–32) can be simplified as

$$\frac{x(s)}{E(s)} = \frac{k_v}{(\tau_e s+1)(ms^2+bs+k) + B_e^2 l^2/R_e s} \cong \frac{k_v\tau_m}{\tau_m s+1} \tag{33}$$

where $k_v = B_e l/R_e$ and $\tau_m = (b + B_e^2 l^2/R_e)/k$. The mass flow rate is given by $\dot{m}_f = \rho v A$, where $A$ is the area of the poppet opening and $\rho$ and $v$ are density and velocity of the fuel, respectively. Here $\dot{m}'_f$ is generated due to $A'$, $v'$, and $\rho'$, which are in turn due to the motion

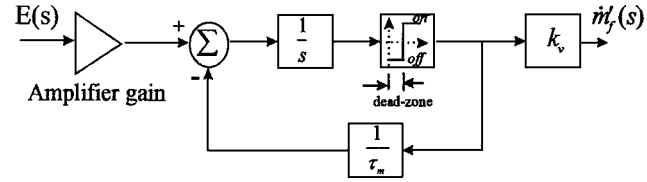


**Fig. 4 Block diagram of a typical two-position injector.**

of the poppet $x$, upstream flow perturbation, and compressibility effects, respectively. This can be expressed as

$$\dot{m}'_f = \rho\bar{A}v' + \rho\bar{v}\bar{A}' + \rho'\bar{A}\bar{v}$$

$$\cong \bar{\rho}\bar{v}A' \tag{34}$$

because the pressure drop across the injector is large due to choked conditions at the outlet and because atomized liquid fuel is assumed to be used for secondary fuel injection. From Eqs. (33) and (34), the fuel injector can be modeled as

$$\frac{\dot{m}'_f(s)}{E(s)} = \frac{k_v k_0 \tau_m \bar{\rho}\bar{v}}{\tau_m s+1} \tag{35}$$

where $k_0 = A/x$. [For more advanced proportional injectors, internal feedback loops exist (for example, using a position transducer for the armature) to guarantee accurate metering and to increase its bandwidth, for example, a Moog DDV proportional valve has a bandwidth of 450 Hz (Ref. 38).]

*2. Two-Position (On–Off) Fuel Injector*

Some fuel injectors currently used for combustion control[11,30,39] operate only between two positions, on and off. Unlike the proportional injectors discussed earlier, the physical stops play a more prominent role in the dynamics. However, one can still model two-position injectors in the same manner as described earlier by including the effect of the physical stops as a saturation block together with Eq. (35), as shown in Fig. 4.

A two-position injector is turned on after the voltage input overcomes a certain threshold, thus creating a dead zone in the control input (Fig. 4), which will be discussed further when control is implemented in Sec. IV.C.

Also note the distinction between the injector dynamics during transition from closing and opening. Typically, the injector is overdriven by a high voltage in the opening mode to ensure fast opening. The opening time constant is different from the closing one because the electromagnetic force is not present during closing. This effect can also be included in the injector model (Fig. 4) by assuming that $\tau_m$ varies between two values $\tau_{m_1}$ and $\tau_{m_2}$ depending on whether the injector is transitioning from off to on or on to off. Note that $\tau_{m_1} = \tau_m$ (as defined before) and $\tau_{m_2} = b/k$. See Ref. 40 for more details regarding this model when validated against two different injectors, Parker 9-130-905 and 9-633-900. (Note that when inertia forces in the armature are important, a second-order fuel-injector model, with high damping is more appropriate. The experimental measurements in Ref. 39 for a General Valve Series 9 model show similar dynamics.)

### B. Actuated Combustor

Denoting the contribution of the fuel injector to the equivalence ratio as $\phi'_c$, we have $\phi'_c = (m'_f/\bar{m}_a)/\alpha_0$, where $\bar{m}_a$ and $\alpha_0$ are the mean air mass flow rate and the stoichiometric fuel to air ratio, respectively. We assume that $\phi'_c$ is uniform radially and that perturbations are carried intact by the mean flow to the burning zone, after a time delay $\tau_c$, where $\tau_c = L_c/\bar{u}$, and where $L_c$ is the distance between the injector discharge and the burning zone and $\bar{u}$ is the mean velocity of the reactants in the combustor.

From Eq. (23), the impact of $\phi'_c$ on the combustion dynamics can be taken into account as

$$\ddot{\eta}_i + 2\zeta\omega_i\dot{\eta}_i + \omega_i^2\eta = (\tilde{b}_i/A_c)[\bar{\kappa}Ru' + d_1\dot{\phi}_c(t-\tau_c)] \tag{36}$$

for $i = 1, 2, \ldots, n$, where $i$ denotes the mode number.

### C. Control Design

*1. Injection at the Burning Zone*

Injection at the flame has shown success in several experimental facilities,[11,29,39] and in a practical full-scale 170 MW gas-turbine combustor.[10] We carry out active control design assuming that the injection is at the flame, using the model in Eq. (36) while $\tau_c \approx 0$, together with the injection dynamics described by Eq. (35). The input–output model relation between the injector input voltage $E$ and the pressure $p'$ is given by

$$p'(s) = W_p(s)E(s), \qquad W_p(s) = k_p Z_p(s)/R_p(s) \tag{37}$$

where $W_p(s)$ is the transfer function of a finite-dimensional model of the combustor and $k_p$, $Z_p(s)$, and $R_p(s)$ are the corresponding gain, numerator, and denominator, respectively.

An appropriate optimal control for the finite-dimensional system as in Eq. (37) is LQG/LTR.[41] Its success lies in its ability to generate satisfactory performance over a wide range of frequencies, unlike phase-shift controllers, which can destabilize stable dynamics.[15,42] Experimental validation of the LQG/LTR for combustion control has been demonstrated in Refs. 26, 40, and 43. In Ref. 26, a similar physically based model was used with a loudspeaker as an actuator. In Refs. 40 and 43, a system-ID approach based on subspace and ARMAX methods[44] was used to suppress pressure oscillations in a dump and a swirl-stabilized combustors, respectively, using pulsed injection. In this paper, we show through simulation studies that LQG/LTR can also be used successfully based on a physical model, using fuel injector as an actuator. For details of the LQG/LTR control design, see Refs. 15 and 26.

Simulations of the LQG/LTR controller were conducted. A fifth-order combustor dynamics model including the first two modes, the flame dynamics, and the injector dynamics is considered. The combustor parameters and conditions are taken as in Ref. 15, which cause a three-quarter-mode instability that resonates at approximately 500 Hz and has unsteady pressure amplitudes of $\mathcal{O}(100\,\text{Pa})$. For this combustor model, an LQG/LTR controller was designed. The fuel injector was assumed to be proportional, with a bandwidth of about 300 Hz, which is achievable with the available injectors.[38] It was also assumed that $\tilde{\phi}_m = |\phi_c'/\bar{\phi}|_{\max} \leq 0.12$ (with $\bar{\phi} = 0.7$). We observed that the resulting controller satisfactorily suppressed the pressure oscillations with a settling time of 10 ms (Ref. 45).

We also carried out a simulation study using an on–off injector. A typical response with an on–off injector is shown in Fig. 5 for a bandwidth of 300 Hz and $\tilde{\phi}_m = 0.125$. When a 300-Hz bandwidth injector was used, the LQG/LTR is still capable of stabilizing the system. We note in Fig. 5 that the pressure is suppressed to a small but finite amplitude limit cycle. The reason is that the injector has a threshold input voltage value at which it is activated. Thus, following the suppression of the instability, the injector stops pulsing

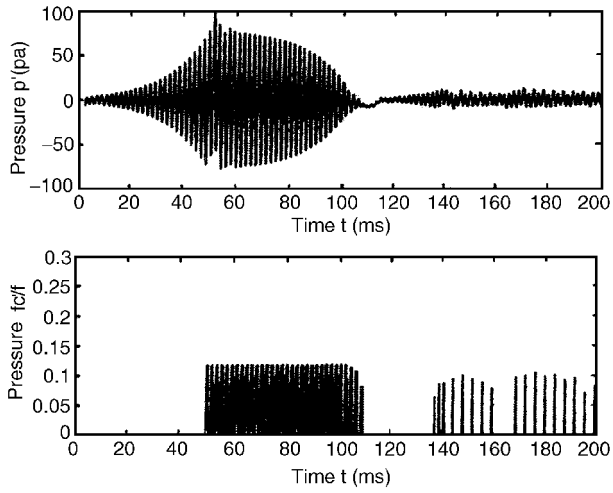


**Fig. 5 Response of the controlled combustor with an on–off injector set to deliver $(\phi_c|_{\max}/\bar{\phi}) \approx 0.125$ and with a bandwidth $\approx 300$ Hz.**

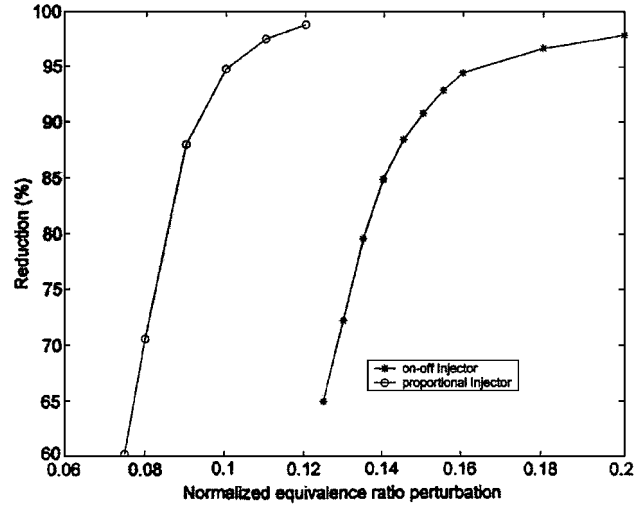


**Fig. 6 Comparison of relative reduction in pressure amplitude using the proportional and on–off injectors with increase in the normalized equivalence ratio perturbation $\tilde{\phi}_m$.**

at from $t \approx 105$ to 138 ms, as seen in Fig. 5. Disturbances in the combustor force the pressure to grow, until the measured voltage by the microphone reaches the threshold at which the injector starts to trigger again. In the case simulated, this occurs at $t > 138$ ms. This sequence is repeated indefinitely.

To quantify the level of achievable reduction in pressure, a quantity $\tilde{p}\%$ was chosen as

$$\tilde{p}\% = \frac{\frac{1}{20}\int_{T_c} \sqrt{p'^2(\tau)}\,\mathrm{d}\tau}{\max_{t\in T}|p'(t)|} \times 100$$

$$T_c = [60\,\text{ms} \quad 80\,\text{ms}], \quad T = [0 \quad 50\,\text{ms}] \tag{38}$$

We chose $T$ as in Eq. (38) because the combustor considered in Ref. 15 reaches its limit-cycle amplitude within this period. $T_c$ was chosen as in Eq. (38) because it represents a typical interval over which control has taken effect. The variation in $\tilde{p}\%$ with $\tilde{\phi}_m$ is shown in Fig. 6 for both the proportional and the on–off injector, for a bandwidth of 300 Hz. At $\tilde{\phi}_m = 0.12$, the proportional injector achieves about 100% reduction, whereas the on–off injector achieves none. As $\tilde{\phi}_m$ was increased to 0.125 and beyond, the on–off injector achieves 65% reduction, which increases gradually with $\tilde{\phi}_m$. (We note that a similar trend in performance was observed in Fig. 13 in Ref. 29.) In contrast, the same levels of reduction can be achieved using the proportional controller for much smaller values of $\tilde{\phi}_m$, between 0.08 and 0.12.

A similar comparison was made between the proportional and on–off injectors on the basis of their bandwidths. As shown in Fig. 7, the bandwidth of the injector basically affects the performance for an on–off injector as opposed to that of a proportional injector. The reason for the latter is that the reduction in achievable output due to a smaller bandwidth is adequately compensated for by the robustness of the LQG/LTR controller to the associated gain and phase changes. Unlike the proportional injector, the on–off injector results in a decreasing amplitude reduction with bandwidth; for bandwidth less than 300 Hz, the on–off injector is simply unable to suppress the pressure oscillations that occur at 500 Hz.

The preceding discussions shows that injector bandwidth is a serious problem.[29,43] Different solutions have been proposed that include 1) developing faster injectors[38] and 2) use of multiple injectors that are fired alternatively to increase the apparent frequency of actuation.[29] A different approach that has shown promise regardless of high-bandwidth injectors is through fuel pulsing at low frequencies (much lower than the acoustics). This is demonstrated experimentally in Refs. 9 and 28 and analytically in Ref. 46.

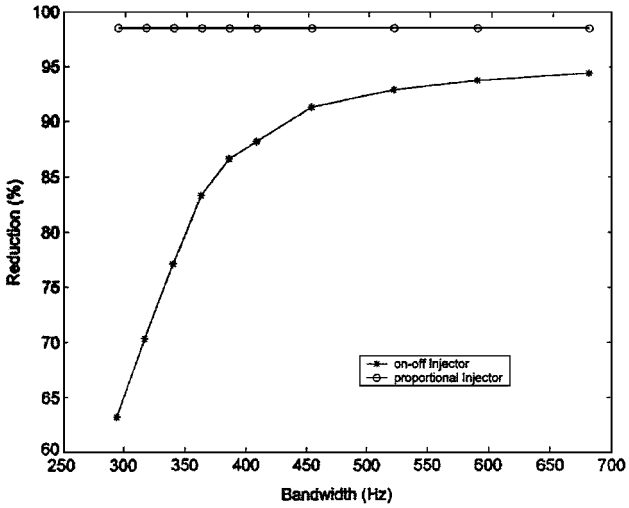


**Fig. 7 Comparison of relative reduction in pressure amplitude using the proportional and on–off injectors with increase in the injector bandwidth; unstable frequency at 500 Hz.**

*2. Injection Upstream the Burning Zone: Delay in the Control Input*

Whereas injecting fuel directly on the flame[10,11,29,39] avoids actuation delays, it introduces hot spots at the flame surface, thus, increasing emissions. In addition, if mixing is weak at the injection port, we run the danger of creating a secondary diffusion flame that can be decoupled from the main premixed flame and, hence, become ineffective in suppressing the instability. [This has been noticed in experiments at Massachusetts Institute of Technology and at UTRC (private communication with J. M. Cohen, 2000).]

In this section, we study pulsed-fuel injection upstream the burning zone. This has been utilized in Ref. 8 where secondary injection was done at the primary fuel source. In Ref. 22, we presented a Posi-Cast control capable of working with an injector located at an arbitrary distance upstream of the flame. In that case, a bulk mode was unstable. Here, we extend the analysis of the Posi-Cast control and show that it is capable of stabilizing longitudinal modes as well.

*3. Posi-Cast Control*

A powerful approach for controlling systems with known time-delay was originated by Smith,[47] which is known as Posi-Cast, for positive forecasting of future states. The idea is to compensate for the delayed output using input values stored over a time window equal to the delay time, that is, $[t-\tau_c, t]$, and to estimate the future output using a model of the combustor. Only stable systems were considered. An extension to include unstable systems was proposed in Ref. 48 using finite-time integrals of the delayed input values, thereby avoiding unstable pole-zero cancellations, which may occur. A frequency-domain pole-placement technique for unstable systems was first proposed in Ref. 49 and a similar technique will be presented here.

The model in Eq. (37), in the presence of a time delay $\tau_c$ can be rewritten as

$$p'(t) = W_p(s)[E(t-\tau_c)], \qquad W_p(s) = \frac{k_p Z_p(s)}{R_p(s)} \tag{39}$$

Because of the nature of the combustion system, not all states are accessible, only the system input, that is, the voltage to the injector $E(t)$, and the output, $p'$ in our case, are measured. A standard pole-placement controller is required. (For more information, see Refs. 49 and 50.) The presence of the time delay $\tau_c$ in the control input motivates the use of an additional signal in the control input $E(t)$, denoted as $E_1(t)$, which anticipates the future output using a model of the system.[22] The resulting controller structure is described as

$$E(t) = [c(s)/\Lambda(s)]E(t-\tau_c) + [d(s)/\Lambda(s)]p'(t) + E_1(t)$$

$$E_1(t) = [n_1(s)/R_p(s)]E(t) - [n_2(s)/R_p(s)]E(t-\tau_c) \tag{40}$$

where $\Lambda(s)$ is a chosen stable polynomial of degree $n-1$; $d(s)$, $n_1(s)$, and $n_2(s)$ are polynomials of degree $n-1$ at most; and $c(s)$ is of degree $n-2$ at most. For stability, these must satisfy the relations

$$c(s)R_p(s) + k_p d(s)Z_p(s) = \Lambda(s)n_2(s) \tag{41}$$

$$n_1(s) = R_p(s) - R_m(s) \tag{42}$$

where $R_m(s)$ is the desired characteristic equation, which is a stable monic polynomial of the same order of $R_p(s)$.

When the controller structure in Eq. (40) is used with the conditions in Eqs. (41) and (42), the closed-loop transfer function can be computed as

$$W_{\mathrm{cl}}(s) = \frac{k_p e^{-s\tau_c}}{R_m(s)} \tag{43}$$

The control input law, in Eq. (40), introduces additional dynamics including nonminimum phase zeros having the same eigenvalues of $R_p(s)$. Obviously, these lead to unstable pole-zero cancellations because the combustor model is open-loop unstable, that is, $R_p(s)$ has unstable eigenvalues. Unstable pole-zero cancellations are known to cause problems concerning observability and controllability of the plant. (See Ref. 36 for more details.) As a result, a modification in the synthesis of $E_1(t)$ in Eq. (40) was suggested by Manitius and Olbrot.[48] To avoid unstable pole-zero cancellations, $E_1(t)$ must be generated as a finite integral of the form

$$E_1(t) = \sum_{i=1}^{n}\left[\int_{-\tau_c}^{0} e^{-\lambda_i\sigma}E(t+\sigma)\,\mathrm{d}\sigma\right] \tag{44}$$

where $\lambda_i$ are the eigenvalues of the combustor system, that is,

$$R_p(s) = \prod_{i=1}^{n}(s-\lambda_i)$$

Taking the Laplace transform of Eq. (44), one can show that

$$\frac{n_1(s)}{R_p(s)} = \sum_{i=1}^{n}\frac{\alpha_i}{s-\lambda_i}, \qquad \frac{n_2(s)}{R_p(s)} = \sum_{i=1}^{n}\frac{\beta_i}{s-\lambda_i} \tag{45}$$

where $\beta_i = \alpha_i e^{\lambda_i\tau_c}$. Another condition for the successful use of the finite integral in Eq. (44) is that $R_p(s)$ has no repeated roots.[49]

The controller described in Eqs. (40) and (44) is sufficient to stabilize the combustor provided that an accurate description of the plant and the time delay are available. This controller has been shown to provide robustness to uncertainties in the plant including the time delay.[48] Adaptive versions of the same controller have been investigated[51,52] and have shown to extend the robustness of the controller to parameter uncertainties.

Simulations of the Posi-Cast controller were conducted. The controller in Eqs. (40) and (44) is implemented for injection at a distance of ~3 cm upstream the burning zone and $\tau_c$ is estimated to be 100 ms, which is about 50 times the time constant of the unstable frequency.

The closed-loop simulation is shown in Fig. 8. Although control is switched on at $t=50$ ms, the pressure keeps increasing for an additional $t=\tau_c=100$ ms (from $t=50$ to 150 ms), then stalls for another 100 ms (from $t=150$ to 250 ms) before decaying. The reason for the former delay is physical and is due to the time taken for the pulsed fuel to reach the burning zone. The latter is due to a computational delay in the controller. Specifically, the finite integral in Eq. (44) outputs incorrect values for a period of $\tau_c$. This is because the computation of the finite integral relies on a stored window of the past values of the control input of the size of $\tau_c$. When control is switched on, the window consists of control inputs proportional to $p'$, which has not yet felt the effect of control due to the physical delay $\tau_c$ (the values of $p'$ are still those of the open-loop combustor). Therefore, it requires $t=2\tau_c$ to start forming a window of integration with control input corresponding to closed-loop values. This confirms observations in Ref. 48.

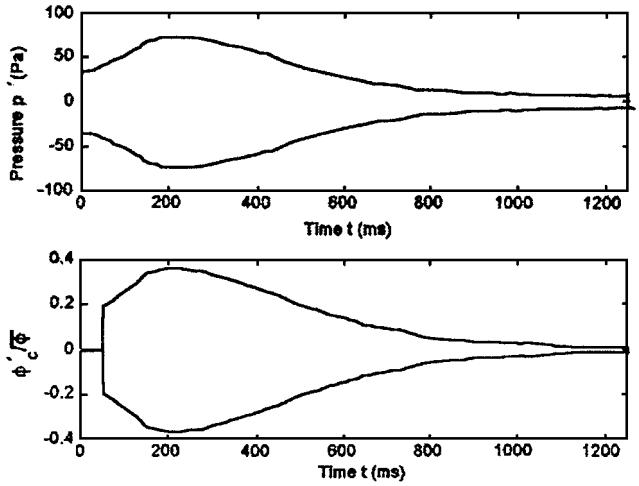


**Fig. 8 Response of the controlled combustor with a time delay of 100 ms in the input signal, proportional injector. Note that only the envelope of the response is shown for clarity because the scale of the plot does not permit seeing individual cycles.**

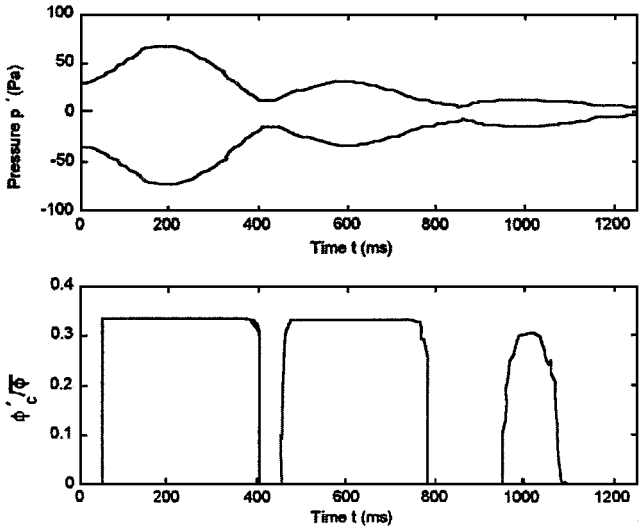


**Fig. 9 Response of the controlled combustor with a time-delay of 100 ms in the input signal, on–off injector. Note that only the envelope of the response is shown for clarity because the scale of the plot does not permit seeing individual cycles.**

In Fig. 9, a two-position injector is used. The control design is based on the linear model, and its parameters are fine tuned to handle the nonlinearities. As discussed earlier, the control is switched on at 50 ms and stabilizes the system. The injector stays on as long as the voltage signal into the injector is greater than a threshold, as discussed before in Sec. IV.A.2.

Note that when combustion instability is caused by $\phi_s'$ fluctuations, as discussed in Sec. II, the characteristic equation looks different than in Eqs. (37) and (39). $R_p(s)$ has terms that are delayed, due to the convective delay $\tau_s$ carried by $\phi_s'$. Hence, $R_p(s)$ becomes infinite dimensional. To circumvent this, a Padé approximation[53] is used to get a finite-dimensional description of $R_p(s)$, and thus, the LQG/LTR and Posi-Cast controllers as described in Secs. IV.C.1 and IV.C.2, respectively, can similarly be used for this case.

## V. Conclusions

Active model-based control of combustion instability is discussed using time-delay models and actuation using fuel injection. The model includes heat-release dynamics, which is characterized using flames with high Damkohler numbers and moderate turbulence responding to perturbations in both the velocity and the equivalence ratio at the burning zone. The time delays present are due to convection and flame propagation, with the former effect due to feedline dynamics convected from the supply to the burning zone and the latter effect due to the reactive mixture propagating at the burning velocity. The convective time delay appears to be the more pronounced effect if equivalence ratio perturbations (which are due to mixing dynamics) are dominant, and the propagation time delay figures prominently when the velocity perturbations at the burning zone are dominant. Interestingly, the time-delay models that are obtained in both cases are similar in form.

We also showed that these time-delay models are able to predict a number of experimental results. The configurations where dominant equivalence ratio perturbations were shown to be present[8,19,20,25] were shown to contain observations similar to the model predictions where equivalence ratio perturbations are dominant. Other configurations, where care was taken to decouple the feedline dynamics from the burning zone by allowing the fuel and air to be thoroughly mixed,[9,23,26–28,35] were also considered. It was shown that the results in these investigations can be corroborated by the model predictions for the case when the velocity perturbations are dominant. Whereas velocity perturbations cause instability even when the time-delay is small because of an inherent phase lag, equivalence-ratio oscillations introduce instability primarily due to a large time delay.

Proceeding toward active model-based control using fuel injection, we first presented a model of a proportional fuel injector by considering its electrical, mechanical, and fluidic components. Based on the combined model of the combustor, the injector, and their interactions, two different control strategies were presented. The first is an LQG-LTR controller, where the effect of time delay is ignored. The second is a Posi-Cast controller that attempts to forecast positively the output at a future instant in the presence of a time delay. The performance of both of these controllers was studied using simulations.

Effects of injection both at and upstream of the burning zone were modeled. The impact of proportional injection was compared and contrasted with an on–off injector. Their performance was discussed with varying authority and bandwidth. It was shown that as the amount of secondary fuel is increased, both proportional and on–off injectors provide increasing pressure reduction, with the former realizing the same values as the latter using 50% smaller amount of fuel. It was also shown that the effect of decreasing bandwidth is minimal on proportional injectors, but significant in the case of on–off injectors. A long-term solution for high performance with active combustion control requires the design of a high-speed, high-authority injector.

## Acknowledgments

This work is sponsored in part by the National Science Foundation Grant ECS 9713415 and in part by the Office of Naval Research Grant N00014-99-1-0448.

## References

[1] Keller, J. O., Vaneveld, L., Koochlet, D., Hubbard, G. L., Ghoniem, A. F., Daily, J. W., and Oppenheim, A. K., "Mechanisms of Instabilities Leading to Flashback," *AIAA Journal*, Vol. 20, 1982, pp. 254–262.

[2] Najm, H. M., and Ghoniem, A. F., "Modeling Pulsating Combustion in Vortex Stabilized Pre-mixed Flames," *Combustion Science Technology*, Vol. 94, 1993, pp. 259–278.

[3] Smith, D. A., and Zukoski, E. E., "Combustion Instability Sustained by Unsteady Vortex Combustion," AIAA Paper 85-1248, 1985.

[4] Kailasanath, K., Gardner, J. H., Oran, E. S., and Boris, J. P., "Numerical Simulation of Unsteady Reactive Flows in a Combustion Chamber," *Combustion and Flame*, Vol. 86, 1991, pp. 115–134.

[5] Bloxsidge, G. J., Dowling, A. P., Hooper, N., and Langhorne, P. J., "Active Control of an Acoustically Driven Combustion Instability," *Journal of Theoretical and Applied Mechanics*, Supplement Vol. 6, 1987.

[6] Zinn, B. T., *Pulsating Combustion. Advanced Combustion Methods*, Academic Press, London, 1986.

[7] McManus, K. R., Poinsot, T., and Candel, S. M., "A Review of Active Control of Combustion Instabilities," *Progress in Energy and Combustion Science*, Vol. 19, 1993, pp. 1–30.

[8] Cohen, J. M., Rey, N. M., Jacobson, C. A., and Anderson, T. J., "Active Control of Combustion Instability in a Liquid-Fueled Low-$NO_x$ Combustor," American Society of Mechanical Engineers, ASME Paper 98-GT-267, 1998.

[9]Richards, G. A., Janus, M. C., Robey, E., Cowell, L., and Rawlins, D., "Control of Flame Oscillations with Equivalence Ratio Modulation," *Journal of Propulsion and Power*, Vol. 15, 1999, pp. 232–240.

[10]Seume, J. R., Vortmeyer, N., Krause, W., Hermann, J., Hantschk, C.-C., Zangl, P., Gleis, S., and Vortmeyer, D., "Application of Active Combustion Instability Control to a Heavy Duty Gas Turbine," *Proceedings of the ASME-ASIA*, 1997.

[11]Murugappan, S., Acharya, S., Gutmark, E., and Messine, T., "Active Control of Combustion Instabilities in Spray Combustion with Swirl," AIAA Paper 2000-1026, 2000.

[12]Rayleigh, J. W. S., *The Theory of Sound*, Vol. 2, Dover, New York, 1945.

[13]Dowling, A. P., and Efowcs, J. E., *Sound and Sources of Sound*, Ellis Horwood, West Sussex, England, U.K., 1983.

[14]Fleifil, M., Annaswamy, A. M., Ghoniem, Z., and Ghoniem, A. F., "Response of a Laminar Premixed Flame to Flow Oscillations: A Kinematic Model and Thermoacoustic Instability Result," *Combustion and Flame*, Vol. 106, 1996, pp. 487–510.

[15]Hathout, J. P., Annaswamy, A. M., Fleifil, M., and Ghoniem, A. F., "A Model-Based Active Control Design for Thermoacoustic Instability," *Combustion Science and Technology*, Vol. 132, May 1998, pp. 99–138.

[16]Peracchio, A. A., and Proscia, W., "Nonlinear Heat Release/Acoustic Model for Thermoacoustic Instability in Lean Premixed Combustors," *ASME Gas Turbine and Aerospace Congress*, American Society of Mechanical Engineers, Fairfield, NJ, 1998.

[17]Dowling, A. P., "Nonlinear Acoustically Coupled Combustion Oscillations," *2nd AIAA/CEAS Aeroacoustics Conference*, May 1996.

[18]Putnam, A. A., *Combustion Driven Oscillations in Industry*, American Elsevier, New York, 1971.

[19]Richards, G. A., and Yip, M. J., "Oscillating Combustion from a Premix Fuel Nozzle," *Combustion Inst./American Flame Research Committee Meeting*, 1995.

[20]Lieuwen, T., and Zinn, B. T., "The Role of Equivalence Ratio Oscillations in Driving Combustion Instabilities in Low $NO_x$ Gas Turbines," *Twenty-Seventh (International) Symposium on Combustion*, Combustion Inst., Pittsburgh, PA, 1998, pp. 1809–1816.

[21]Fleifil, M., Hathout, J. P., Annaswamy, A. M., and Ghoniem, A. F., "Reduced-Order Modeling of Heat Release Dynamics and Active Control of Time-Delay Instability," AIAA Paper 2000-0708, Jan. 2000.

[22]Hathout, J. P., Fleifil, M., Annaswamy, A. M., and Ghoniem, A. F., "Heat-Release Actuation for Control of Mixtureinhomogeneity-Driven Combustion Instability," *Twenty-Eighth (International) Combustion Symposium*, Combustion Inst., Pittsburgh, PA, 2000.

[23]Lang, W., Poinsot, T., and Candel, S., "Active Control of Combustion Instability," *Combustion and Flame*, Vol. 70, 1987, pp. 281–289.

[24]Annaswamy, A. M., Fleifil, M., Hathout, J. P., and Ghoniem, A. F., "Impact of Linear Coupling on the Design of Active Controllers for Thermoacoustic Instability," *Combustion Science and Technology*, Vol. 128, Dec. 1997, pp. 131–180.

[25]Mongia, R., Dibble, R., and Lovett, J., "Measurement of Air-Fuel Ratio Fluctuations Caused by Combustor Driven Oscillations," American Society of Mechanical Engineers, ASME Paper 98-GT-304, 1998.

[26]Annaswamy, A. M., Fleifil, M., Rumsey, J., Hathout, J. P., Prasanth, R., and Ghoniem, A. F., "Thermoacoustic Instability: Model-Based Optimal Control Designs and Experimental Validation," *IEEE Transactions on Control Systems Technology*, 2000.

[27]Gulati, A., and Mani, R., "Active Control of Unsteady Combustion-Induced Oscillations," *Journal of Propulsion and Power*, Vol. 8, No. 5, 1992, pp. 1109–1115.

[28]Sivasegaram, S., and Whitelaw, J. H., "Active Control of Oscillations in Combustors with Several Frequency Modes," Proceedings of the ASME Winter Annual Meeting, American Society of Mechanical Engineers, Fairfield, NJ, 1992.

[29]Yu, K., Wilson, K. J., and Schadow, K. C., "Scaleup Experiments on Liquid-Fueled Active Combustion Control," AIAA Paper 98-3211, 1998.

[30]Hathout, J. P., Fleifil, M., Annaswamy, A. M., and Ghoniem, A. F., "Role of Actuation in Combustion Control," 1999 Inst. of Electrical and Electronics Engineers CCA/CACSD, Aug. 1999.

[31]Dowling, A. P., "A Kinematic Model of of a Ducted Flame," *Journal of Fluid Mechanics*, Vol. 394, 1999, pp. 51–72.

[32]Schadow, K. C., Gutmark, E., Parr, T. P., and Wilson, K. J., "Passive Shear Flow Control to Minimize Ramjet Instabilities," *23rd JANNAF Combustion Meeting*, 1986.

[33]Yang, V., and Anderson, R. (eds.), *Liquid Rocket Engine Combustion Instability,* Progress in Astronautics and Aeronautics, AIAA, Washington, DC, 1995.

[34]Niculescu, S. I., Annaswamy, A. M., Hathout, J. P., and Ghoniem, A. F., "Control of Time-Delay Induced Instabilities in Combustion Systems," *Proceedings of the IFAC Workshop on System Structure & Control*, 2001.

[35]Kim, K., Lee, J., Stenzler, J., and Santavicca, D. A., "Optimization of Active Control Systems for Suppressing Combustion Dynamics." *RTO Symposium on Active Control Technology for Enhanced Performance Operational Capabilities of Military Aircraft*, 2000.

[36]Ogata, K., *Modern Control Engineering*, 3rd ed., Prentice–Hall, Upper Saddle River, NJ, 1997.

[37]Meirovitch, L., *Elements of Vibration Analysis,* 2nd ed., McGraw–Hill, New York, 1986.

[38]Hantschk, C., Hermann, J., and Vortmeyer, D., "Active Instability Control with Direct Drive Servo Valves in Liquid-Fuelled Combustion Systems," *Proceedings of the International Symposium on Combustion*, 1996.

[39]Magill, J. C., Bachmann, M., and McManus, K. R., "Combustion Instabilitydynamics and Control in Liquid-Fueled Direct Injection Systems Suppression in Liquid-Fueled Combustors," AIAA Paper 2000-1022, 2000.

[40]Brunell, B. J., "A System Identification Approach to Active Control of Thermoacoustic Instabilities," M.S. Thesis, Massachusetts Inst. of Technology, Cambridge, MA, 2000.

[41]Stein, G., and Athans, M., "The LQG/LTR Procedure for Multivariable Feedback Control Design," *IEEE Transactions on Automatic Control*, Vol. 32, Feb. 1987, pp. 105–114.

[42]Fleifil, M., Annaswamy, A. M., Hathout, J. P., and Ghoniem, A. F., "The Origin of Secondary Peaks with Active Control of Thermoacoustic Instability," *Combustion Science and Technology*, Vol. 133, June 1998, pp. 227–260.

[43]Murugappan, S., Park, S., Acharya, S., Annaswamy, A. M., Gutmark, E., and Ghoniem, A.F., "Optimal Control of Swirl-Stabilized Combustor Using a System Identification Based Model," Turbine 2000, 2000.

[44]Ljung, L., *System Identification: Theory for the User,* Prentice–Hall, Englewood Cliffs, NJ, 1987.

[45]Hathout, J. P., Annaswamy, A. M., and Ghoniem, A. F., "Modeling and Control of Combustion Instability Using Fuel Injection," *RTO Symposium on Active Control Technology for Enhanced Performance Operational Capabilities of Military Aircraft*, 2000.

[46]Prasanth, R., Annaswamy, A. M., Hathout, J. P., and Ghoniem, A. F., "When Do Open-Loop Strategies for Combustion Control Work?," AIAA Joint Propulsion Conf. (to be published).

[47]Smith, O. J., "A Controller to Overcome Dead Time," *ISA Journal*, Vol. 6, 1959.

[48]Manitius, A. Z., and Olbrot, A. W., "Finite Spectrum Assignement Problem for Systems with Delays," *IEEE Transactions on Automatic Control*, Vol. AC-24, No. 4, 1979.

[49]Ichikawa, K., "Frequency-Domain Pole Assignment and Exact Model-Matching for Delay Systems," *International Journal of Control*, Vol. 41, 1985, pp. 1015–1024.

[50]Wolovich, W. A., *Linear Multivariable Systems,* Springer-Verlag, Berlin, 1974.

[51]Ortega, R., and Lozano, R., "Globally Stable Adaptive Controller for Systems with Delay," *International Journal of Control*, Vol. 47, No. 1, 1988, pp. 17–23.

[52]Niculescu, S. I., and Annaswamy, A. M., "A Simple Adaptive Controller for Positive-Real Systems with Time-Delay," *American Control Conference* (to be published).

[53]Baker, G. A., and Graves-Morris, P., *Padé Approximants*, Cambridge Univ. Press, 2nd ed., Cambridge, England, U.K., 1996.